HUNTINGTON MEDICAL RESEARCH INSTITUTES

NEUROLOGICAL RESEARCH LABORATORY

734 Fairmount Avenue

Pasadena, California 91105

Contract No. NO1-NS-5-2333

QUARTERLY PROGRESS REPORT

January 1 - March 31, 1996

Report No. 2

"MICROSTIMULATION OF THE LUMBOSACRAL SPINAL CORD"

William F. Agnew, Ph.D.

Randy R. Carter, Ph.D.

Barbara Woodford, Ph.D.

Douglas B. McCreery, Ph.D.

Leo A. Bullara, B.A.

This QPR is being sent to you before it has been reviewed by the staff of the Neural Prosthesis Program.

Abstract

In this quarter, we report on four chronic experiments aimed at examination of the effects of chronic electrical stimulation on spinal cord tissue. One array developed current leaks, preventing stimulation and in another the cat severed the lead wires at the mid-thoracic level. The remaining two experiments were completed with the results indicating that pulsing of the electrodes with continuous stimulation (20 Hz, 80 μA, 400 μsec/phase, 32 nC/phase, 3,200 μC/cm^2) applied in two 12-hour periods caused minimal depression of neuronal excitability. We emphasize that the duty cycle and duration of stimulation used in this study was more rigorous than that anticipated for neuroprosthetic applications of spinal cord stimulation.

In one animal (SP-58), histology indicated that the number of blood-borne monocytes surrounding the stimulating tip of one of the pulsed electrodes was greater than that surrounding an unpulsed electrode. Otherwise, histopathology, including aseptic inflammation, was similar to that reported in chronic implants without continuous stimulation. In the second animal (SP-61), blood-borne monocytes and active macrophages were associated almost equally with all electrodes, pulsed or unpulsed. However, in this animal, the electrode tips were all within 1 mm of each other, which may have contributed to the ambiguous results. Our preliminary conclusion is that continuous stimulation may enhance inflammatory processes initiated by the implantation of microelectrodes.

We also report the results of three acute experiments. In two, a novel surgical approach was attempted. In the other, repeatable, complete bladder/urethral pressure profiles were taken. This technique generated repeatable pressure measures and will be used to determine the effects of spinal cord stimulation and pharmacologic agents.

Introduction

The overall goals of this contract are to develop a method of chronic microstimulation of the sacral cord of the cat to effect micturition, and to evaluate the effects of the electrical stimulation on neural and surrounding tissues. In this report we discuss the results from two chronic experiments in which microelectrodes implanted in the spinal cord for 3-4 weeks were chronically stimulated (12 hrs continuous stimulation on 2 successive days). Physiologic results demonstrated that this chronic stimulation only slightly depressed neuronal excitability. Histologic results suggested that chronic stimulation may enhance the inflammatory response to the resident microelectrodes.

Three acute experiments have been performed this quarter to improve our methodology. Two experiments were designed to evaluate a new surgical approach that could shorten both the duration of the implant surgery and subsequent animal recovery. This technique has merit but will require a modified method of localizing the S_2 segment of the cord. In the other acute experiment, a constant velocity motor was used to slowly withdraw a solid-state pressure sensor from inside the bladder along the complete length of the urethra. Results indicate that this technique provides repeatable bladder/urethral pressure profiles providing information about all positions along this length rather than at only two points as in our previous recordings. This method measures direct hydrostatic pressure rather than relying on indirect measures using saline infusion.

Methods

Chronic Experiments. Adult male cats were anesthetized with 50% nitrous oxide and 1-2% Halothane and the spinal cord exposed as described previously. The S_2 region of the spinal cord was localized by stimulation of the dermatome it serves while recording the dorsal cord potential supradurally, as described previously. No substrate was used to support the electrodes. Four activated iridium microelectrodes (50 μm dia., 2.8 mm long, 2000 μm^2 exposed stimulating surface) were implanted manually at approximately the dorsal midline of the spinal cord and angled outward at about 10 degrees. The electrodes were pulsed individually and the bladder lumen pressure and intraurethral tone were monitored. The electrodes were advanced into the cord until good elevation of bladder pressure was produced by the stimulation. The dura was

then closed over the electrodes and the effect of the stimulation again measured. A silastic pad (to which the stimulating electrode leads had been glued) was sutured to the dura to reduce traction on the electrodes. The ground electrode was sutured in place over the microelectrodes. A small hole was made in the dura and a recording electrode inserted and threaded so as to lie approximately 3 cm caudal to the stimulating electrodes. A suture was used to secure the recording electrode to the dura. A reference electrode was sutured to the muscle 2 cm above the dura. The wound was flushed with antibacterial solution and the muscle and skin were closed in layers. Subsequent recordings were made with the animal anesthetized with Pentothal (i.v., as needed) or Nembutal (i.v., as needed). A sterile catheter and sterile saline were used during recording of the bladder lumenal pressure.

After functional electrodes had been implanted for 3-4 weeks, the cats were anesthetized with Propofol (0.5-2.0 ml/hr) and chronic stimulation was initiated. This protocol called for continuous stimulation for 12 hours/day for two consecutive days. The animal's core temperature was monitored and maintained at approximately 38 C using a heating pad and radiant heat lamp. Normal saline or lactated ringers solution was administered (iv) as needed to maintain adequate hydration.

Acute Experiments. Three adult male cats were anesthetized with 50% nitrous oxide and 1-2% Halothane. In two cats, the spinal cord was exposed by drilling a 3 mm by 5 mm hole through the side of vertebra L6. Our intent was to explore the possibility of exposing the cord using a less traumatic means to speed both the surgery and subsequent recovery. In the remaining cat, the cord was exposed using a standard full dorsal laminectomy. In all cases, the S_2 region was localized in the manner described above. The spinal cord was covered with light mineral oil to prevent drying. The stimulating electrodes were inserted into the cord using a standard stereotaxic apparatus.

In one cat, a small (transducer ~1.3 mm dia, catheter ~0.8 mm dia) pressure transducer (Millar Instruments) was passed along the length of the urethra and then slowly withdrawn at a constant rate using an electric motor. The frequency response of this pressure transducer is flat to 10 KHz. A potentiometer coupled to the shaft of the motor allowed measurement of the distance the catheter was withdrawn as a function of time. Both the pressure and position signals were

digitally stored on tape (18.5 KHz sampling rate per channel). These signals were then digitized off-line at 10 Hz per channel for further analysis.

Histology. Within 20 minutes of the end of an experiment the animal was anesthetized with Nembutal and perfused through the aorta with saline followed by 2 L of 1/2 strength Karnovsky's fixative (2% paraformaldehyde and 2.5% glutaraldehyde) in 0.1 M sodium cacodylate buffer, pH 7.4. With the electrodes *in situ*, the complete cord and spinal roots were dissected out to precisely localize the microelectrodes. Two-mm-thick transverse sections containing the electrode tracks were dissected, processed and embedded in epoxy resin. One-μm thick sections were cut serially through the blocks and examined using light microscopy. In SP-58, transverse sections of the tips of electrodes 1 and 4 were cut into ultrathin sections and observed with the electron microscope. In SP-61, the proximity of the tips did not allow for thin sectioning and electron microscopy.

Results

The results from chronic experiments have been mixed. Of the four chronic experiments initiated, only two were completed (SP-58 and SP-61). In a third (SP-59), the electrode assembly developed current leaks and that chronic stimulation was not possible. In the fourth (SP-60), the cables connecting the electrode array and the percutaneous connector on the head were severed at the mid-thoracic level. Animal care personnel reported that this animal, while restricted to its cage, was often seen rolling on his back. It is felt that this is the likely cause of the break since we have not encountered a similar problem in any other animal.

Histologic Results. In SP-58, electrodes 2 and 3 were found shallow and angled laterally so that the tips were likely outside the cord proper (Fig. 1 and Fig. 2). The sites of electrodes 1 and 4 were examined with electron microscopy. Dark mononuclear cells surrounded the tip of electrode 4, which was in the left ventro-medial ventral horn (Fig. 3A). Electrode 1 passed through the left PPN, and the tip was found in the ventral intermediate gray (Fig. 3B). Light microscopy showed that the dark cells around the tip of electrode 4 were probably blood-borne monocytes and/or microglia with few inclusions (Fig. 4A and B), indicating that they were recently recruited to the site. In contrast, fully active macrophages found more dorsally along the track contained both dense and vacuolar inclusions (Fig. 4C). The difference can be seen more

clearly in the electron micrographs of the cells near the tip of electrode 4 (Fig. 5) and the cells along the shaft (Fig. 6). Normal-appearing neuronal cell bodies were found within 150 μm from the focus of monocytes around the tip (Fig. 4A). The tracks of electrodes 4 and 1 were irregularly bordered near the tip, suggesting that the tissue had been avulsed when the electrodes were removed from the cord (Fig. 3). In addition, the termination of both tracks contained dark amorphous extracellular material and fragmented cells with indistinct cell membranes, as seen in Figures 3 and 7.

Monocytic cells, mostly active macrophages, were found near the tip of electrode 1 (Figs. 8, 9A, 10). Adjacent perivascular cuffing of activated monocytes corroborates the blood-borne nature of the cells in tissue around the tip (Fig. 11). The dark areas (Fig. 8C) were not mononuclear cells but were portions of the lateral funiculus enclosed by the intermediate gray near the electrode tip (Fig. 9D). Myelinated axons adjacent to the tip were of small caliber. Lateral to electrode 1 was a narrow scar containing fibroblasts or elongated glial cells, indicating medio-lateral movement of the electrode within the cord (Fig. 9B). Several of the nuclei of the PPN showed minor signs of chromatolysis, such as indented nuclei, peripheral RER, and filamentous cytoplasm (Adams et al., 1984). There were also many lipofuscin bodies, commonly found in aging animals (Figs. 9C and 12).

In SP-61, all the electrodes were within a 1 mm segment (Fig. 13) and electrodes 1 and 3 had been pulsed. All of the electrode tips were associated with disorganized tissue containing monocytes and/or microglia, cellular debris, and macrophages (Figs. 14 and 15). The tissue around electrode 3 contained many dark monocytic cells, as described for electrode 4 of SP-58 (Fig. 15A and B), but there were also full-fledged macrophages. Two of the electrode tracks were close to the central canal, and its ependymal cells were damaged, but there were no signs of scarring suggesting movement of the electrodes. The tips of electrode pairs 1 and 2, and 3 and 4 were 100 μm or less apart.

Physiologic Results. After the electrode array had been implanted for three weeks, electrodes 2 and 4 of cat SP-58 were stimulated continuously at 20 Hz, 80 μA, 400 μsec/phase, 32 nC/phase, 3,200 $\mu C/cm^2$ (cathodic first) for 12 hours on each of two successive days. The other electrodes served as unstimulated controls. Figure 16 shows the amplitude of the average evoked compound action potential (AECAP) as a function of the stimulus amplitude. The curves

were generated before the start of the stimulation, at the end of the first 12 hour stimulation period, and at the end of the second 12 hours of stimulation. There may have been a slight depression of neuronal excitability. The results for electrode 2 were very similar but no there was no evidence of any depression. Overall, this animal showed no significant difference before, during, or after the chronic stimulation period.

In SP-61, the electrode arrays had been implanted for 4 weeks when chronic stimulation was initiated. Electrodes 1 and 3 were pulsed continuously at 20 Hz, 80 μA, 400 μsec/phase (cathodic first) for 12 hours on each of two successive days. Figure 17 shows the recruitment curves for electrode 1. At the end of the first 12 hour stimulation period, the evoked potential actually increased slightly at each stimulus amplitude suggesting an increase in neuronal excitability. At the beginning of the second 12 hour session, this increased excitability remained but was depressed by the end of the second 12 hours of stimulation. Overall, these changes are considered minor given the extended periods of stimulation at what would be considered functional amplitudes.

Figure 18 shows the response evoked by electrode 3. After the first 12 hour period, neuronal excitability was slightly depressed at the lower stimulation amplitudes and the threshold had shifted from 1-2 μA to 9-10 μA. This had changed very little as can be seen in the response prior to beginning the second stimulation period. After the second 12 hour period, the recruitment curve was again somewhat depressed.

In two acute experiments (SP-62, SP-63), a new surgical approach was attempted. A complete dorsal laminectomy involving several cord levels is time consuming for the surgeon and has significant recovery time for the animal. A new procedure was attempted in which a high-speed drill was used to open a "window" through the side of a single vertebra. The dura was incised and electrodes were inserted through the opening. While promising, there were difficulties with this method. First, localization of the S_2 cord segment was more difficult since the recording electrode cannot be slid up and down the cord dorsum. There was signal spread and distortion introduced by the presence of the bone and muscle. Second, it was not possible to visualize (and hopefully avoid) the large blood vessels on the surface of the cord. This may not be a significant problem if the electrodes are inserted from a more lateral angle. On the positive side, this procedure was much faster than our previous technique.

In a third acute experiment (SP-64), a small pressure transducer was inserted into the bladder and withdrawn slowly (1.54 cm/s) using a constant velocity motor. The computer recorded the pressure as a function of time and the voltage across a potentiometer linked to the shaft of the motor as a function of time. Figure 19 displays six successive bladder/urethral pressure profiles as a function of distance from the tip of the penis. The range 0-3.5 cm is within the penis and the pressure peak at about 4 cm corresponds to the level of the bulbocavernosus and ishiocavernosus muscles. The distance 4.5-6.3 cm corresponds to the external urethral sphincter muscle. Above this level corresponds to the bladder neck and lumen. The pressure profile showed no clear indication of the internal sphincter muscle. Overall, it was felt that the response is quite repeatable and should be a useful technique in attempting to clarify how spinal cord stimulation or pharmacologic agents affect the urologic system.

Discussion

With histologic results from only two animals, it is too early to come to any conclusion about the effects of continuous stimulation on the spinal cord. The pulsing parameters used with these two animals was of an amplitude known to produce significant bladder pressure elevation but was delivered continuously during two 12 hour periods. Under these conditions, some electrically-induced damage would not have been surprising. However, the relatively low frequency (20 Hz) may have reduced the risk of tissue injury. All the tips examined were in the gray matter and, by light microscopy, no damage to the neuronal cell bodies could be definitively attributed to the stimulation above that typically noted surrounding chronically implanted, but unpulsed, electrodes. We did not observe any shrunken hyperchromic neurons as we have seen in stimulated cerebral cortex. The presence of chromatolysis in neurons indicates that axons have been damaged, a feature hardly avoidable with the insertion of a sharp object and not necessarily a prognosticator of cell death.

However, the exaggeration of an inflammatory response, as demonstrated by the invasion of blood-borne macrophages at the sites of stimulation, raises the possibility that macrophage-induced cytotoxicity might damage the gray matter. Unfortunately, the results of SP-61 were unable to be corroborated by electron microscopy. Thus, it is not clear if this monocytic invasion is a consistent effect of stimulation. It may be that, since pairs of pulsed and unpulsed tips were

within 100 μm of each other, monocytic migration to the pulsed electrodes may have included invasion of the tissue around the unpulsed tip as well.

The loose fragmented tissue at the electrode tips (Figs. 3, 7, 14, and 15) may have resulted from explantation of the electrodes and may not be related to pulsing of the microelectrodes.

It currently appears that the effects of chronic implantation of the electrode such as diffuse and focal axonal degeneration, aseptic inflammation, glial or fibrocytic ensheathment, and fragmented structures in gray matter (Woodford, et al, 1996) are more severe than the effects of chronic stimulation in the sacral spinal cord.

The physiologic results of the 24 hour stimulation experiments are encouraging. The stimulation protocol employed a combination of amplitude, frequency, and pulse width that produced significant increases in bladder lumenal pressure in previous experiments.

The modified surgical procedure offers benefits but also points out potential drawbacks. This technique shortens both the time required to perform the surgery and the subsequent recovery. This would be of significant benefit when applied in human patients since it should lead directly to lower surgical risk and better tolerance by a wider range of patients. On the other hand, this method makes it more difficult to accurately localize the desired position for electrode placement. Also, it is not possible to visualize blood vessels lying on the surface of the cord. We will consider further modification of our surgical approach in attempting to overcome this limitations.

A new approach was used to measure the pressure within the bladder and along the urethra. Measuring the pressure directly rather than relying on indirect back-pressure during saline infusion is a significant improvement. In previous experiments we recorded the bladder pressure in 0.5 cm increments using this same small pressure transducer. Using a constant velocity motor makes this process much easier. The transducer was withdrawn slowly since tactile stimulation of the urethral wall may reinforce bladder contractions (Barrington, 1921; 1925; 1931; 1941). We feel that such reflex stimulation was minimal due to the slow speed of withdrawal and the small size of the transducer (~ 1.3 mm dia) and the catheter (~ 0.8 mm dia). On the other hand, the speed should be fast enough to travel the entire length of the urethra in a period shorter than one would expect state changes to occur. For example, the bladder pressure response to spinal cord stimulation may fatigue after 20-30 s depending on the stimulus rate and

duty cycle. We felt that withdrawing the transducer over a period of approximately 10 s was an appropriate compromise and, in fact, successive trials were quite repeatable.

Future work

In the next quarter we plan to continue chronic studies aimed at evaluating the response of the spinal cord to chronic stimulation using both light and electron microscopy. Work will also continue on new electrode configurations and improved positional stability of chronic spinal cord arrays. Additional acute experiments will be conducted to further examine the effects of stimulation along the entire bladder/urethral length.

References

Adams, JH, Corsellis, JAN, and Duchen, LW (eds.) General pathology of neurons and neuroglia, Greenfield's Neuropathology, 4th ed., John Wiley & Sons, New York (1984) 20-22.

Barrington, FJF. The relation of the hindbrain to micturition, *Brain*, 44 (1921) 23-53.

Barrington, FJF. The effect of lesion of the hind- and midbrain on micturition in the cat, *Quart. J. Exp. Physiol.*, 15 (1925) 81-102.

Barrington, FJF. The component reflexes of micturition in the cat, Parts I and II, *Brain*, 54 (1931) 177-188.

Barrington, FJF. The component reflexes of micturition in the cat, Part III, *Brain*, 64 (1941) 239-243.

Woodford, BJ, Carter, RR, McCreery, DB, Bullara, LA, Agnew, WF. Histopathologic and physiologic effects of chronic implantation of microelectrodes in sacral spinal cord of the cat, In review, J Neuropath and Exp Neurol.

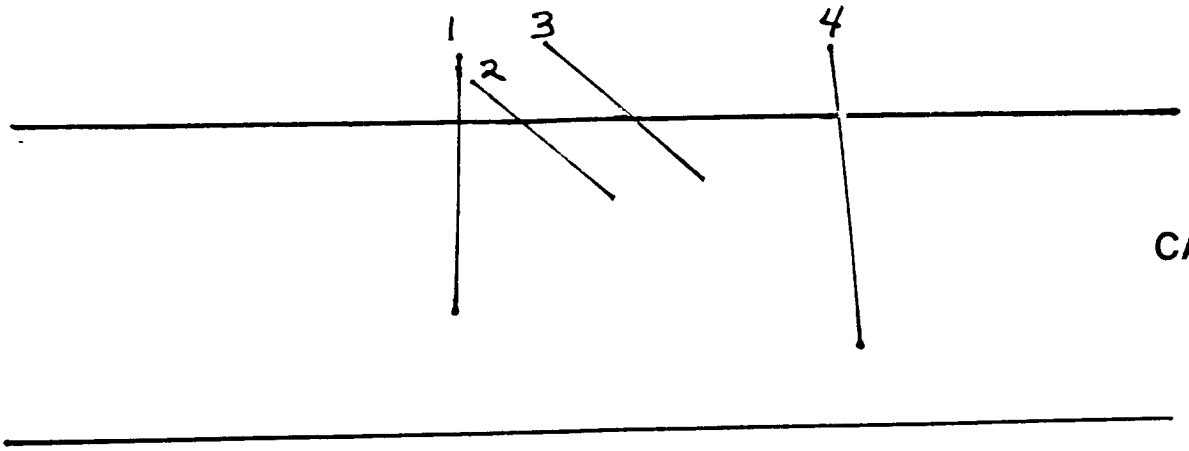

ROSTRAL

CAUDAL

A.

Longitudinal

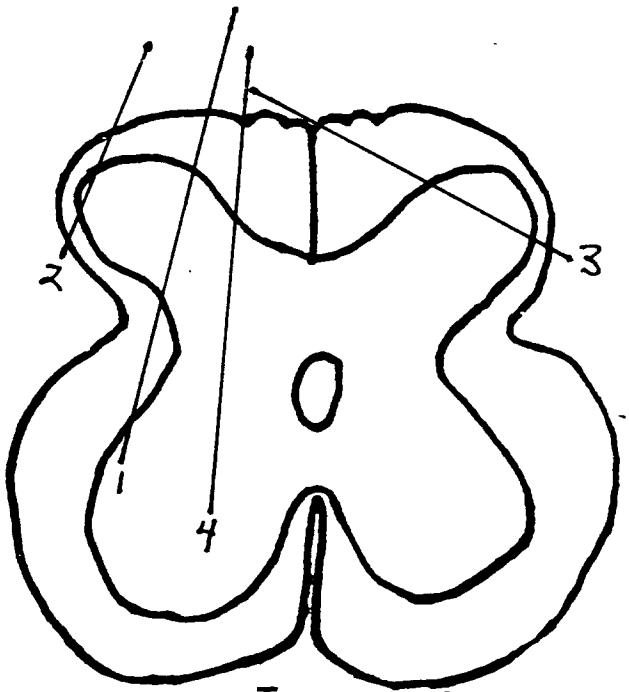

Transverse

B.

S2

SP58

A. Longitudinal reconstruction of location of electrode tracks in serial sections, showing rostral-caudal angles and tip depths. **B.** Transverse view of electrode tracks in serial sections, showing medial-lateral angles and tip positions in relation to PPN. Electrodes 2 and 4 were pulsed continuously.

Figure 1

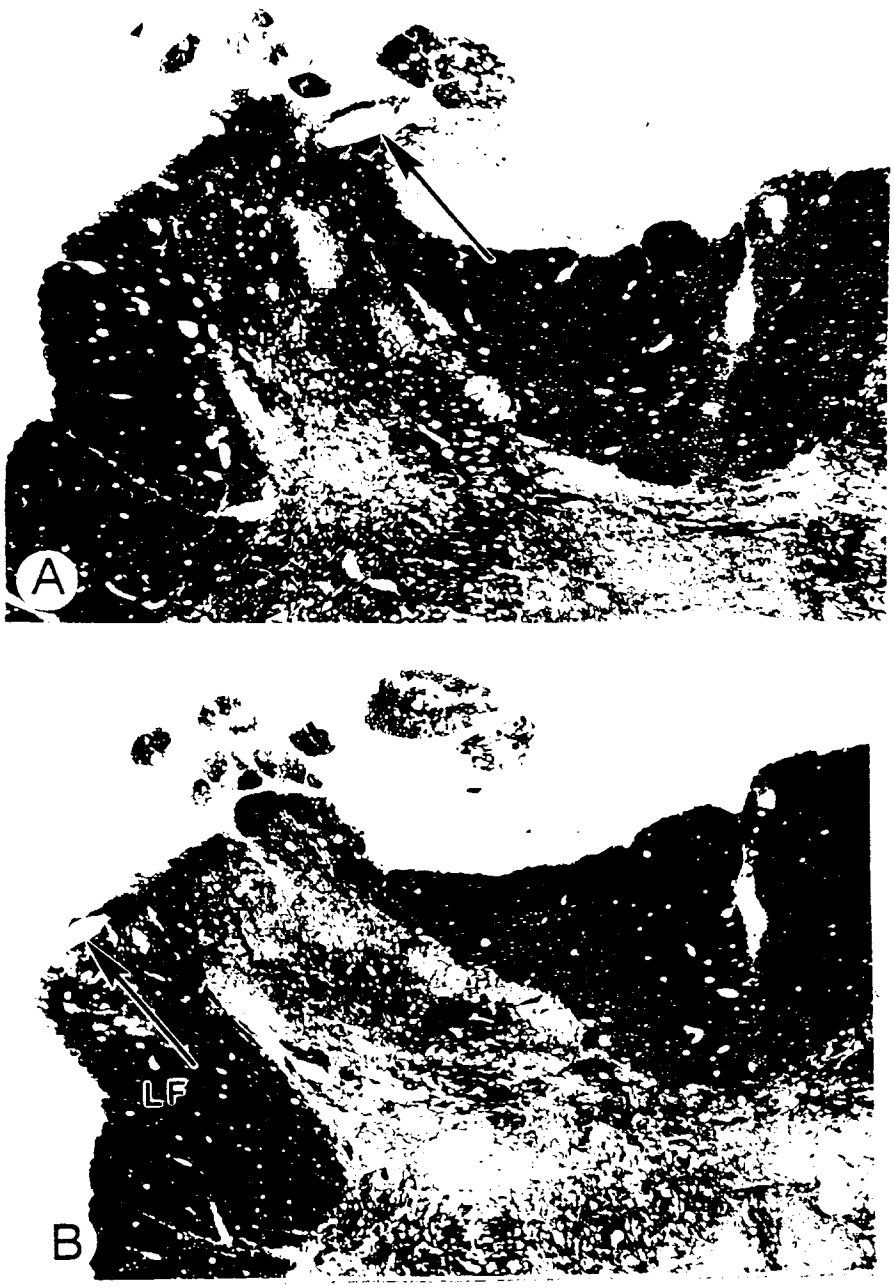

Fig. 2. SP-58, electrode 4. A. The track of the electrode (arrow) enters the dorsal surface of the spinal cord at an extreme angle. B. Many serial sections further, the track (arrow) exits the cord at the dorsal lateral funiculus (LF). X 34.

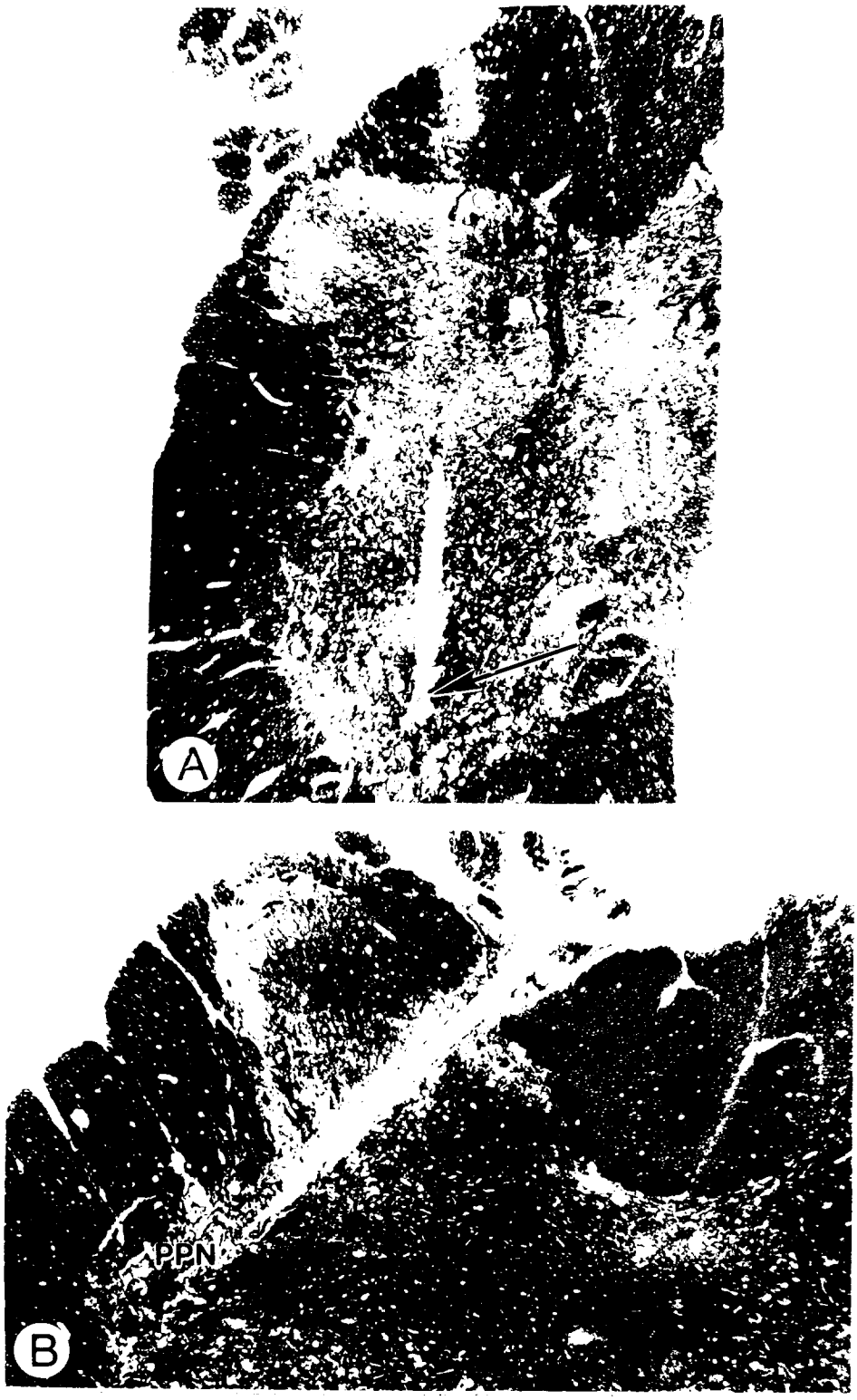

Fig. 3. SP-58. A. Pulsed electrode 4 passes through the intermediate gray, and the tip is in the left ventro-medial horn (arrow). B. The tip of unpulsed electrode 1 is in the parasympathetic preganglionic nucleus (PPN). X 34.

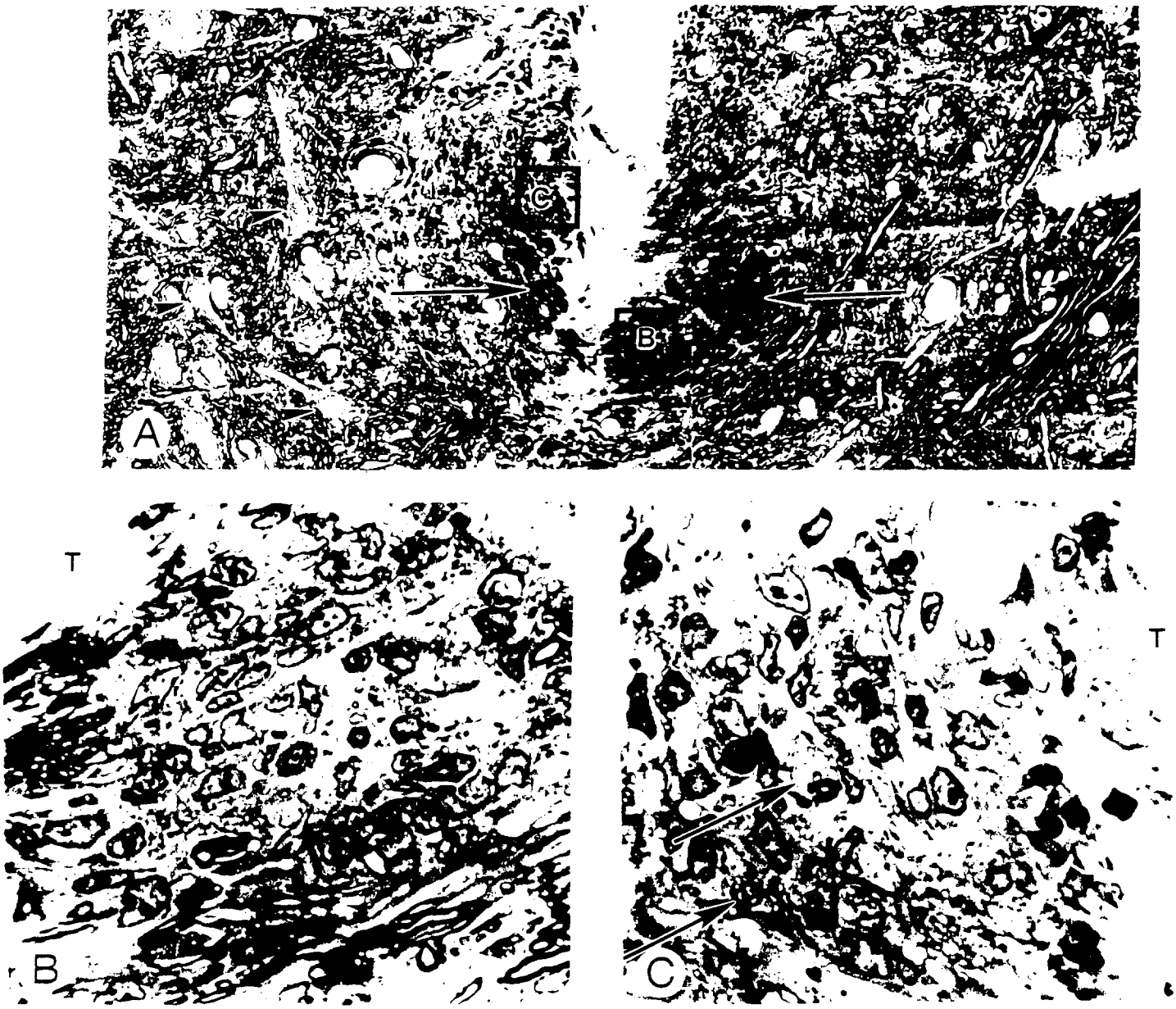

Fig. 4. SP-58, electrode 4. A. The tip of electrode 4 is bordered on both sides by dark mononuclear cells (arrows). Note the normal-appearing neuronal cell bodies about 150 µm outside the periphery of these dark cells (arrowheads). X 170. B. Higher magnification of the mononuclear cells medial to the track (T) at the tip in A. X 850. C. Higher magnification of cells lateral to the shaft track (T) in A. Note that many of these cells have phagocytic inclusions (arrows). X 850.

Fig. 5. Electron micrograph of cells at tip of SP-58, electrode 4. Note that these cells are mononuclear with few phagocytic inclusions. They have no filaments or basal lamina, suggesting that they are blood-borne monocytes or microglia. X 13,200.

Fig. 6. Electron micrograph of macrophages along lateral shaft of SP-58, electrode 4, such as Fig. 4C. These cells have many inclusions, including myelinated debris, suggesting that they have been phagocytic for more than several days. X 6,800.

Fig. 7. Electron micrograph of dark amorphous extracellular material at the ventral tip of SP-58, electrode 4. The cell structures lack distinct membranes (arrows). X 6,800.

Fig. 8. SP-58, electrode 1. The unpulsed electrode passes through the lateral intermediate gray, the location of the parasympathetic preganglionic nucleus. The edges of the track are irregular, suggesting avulsion of the tissue during extraction of the electrode. Areas A, B, C and D are enlarged in Fig. 9. X 170.

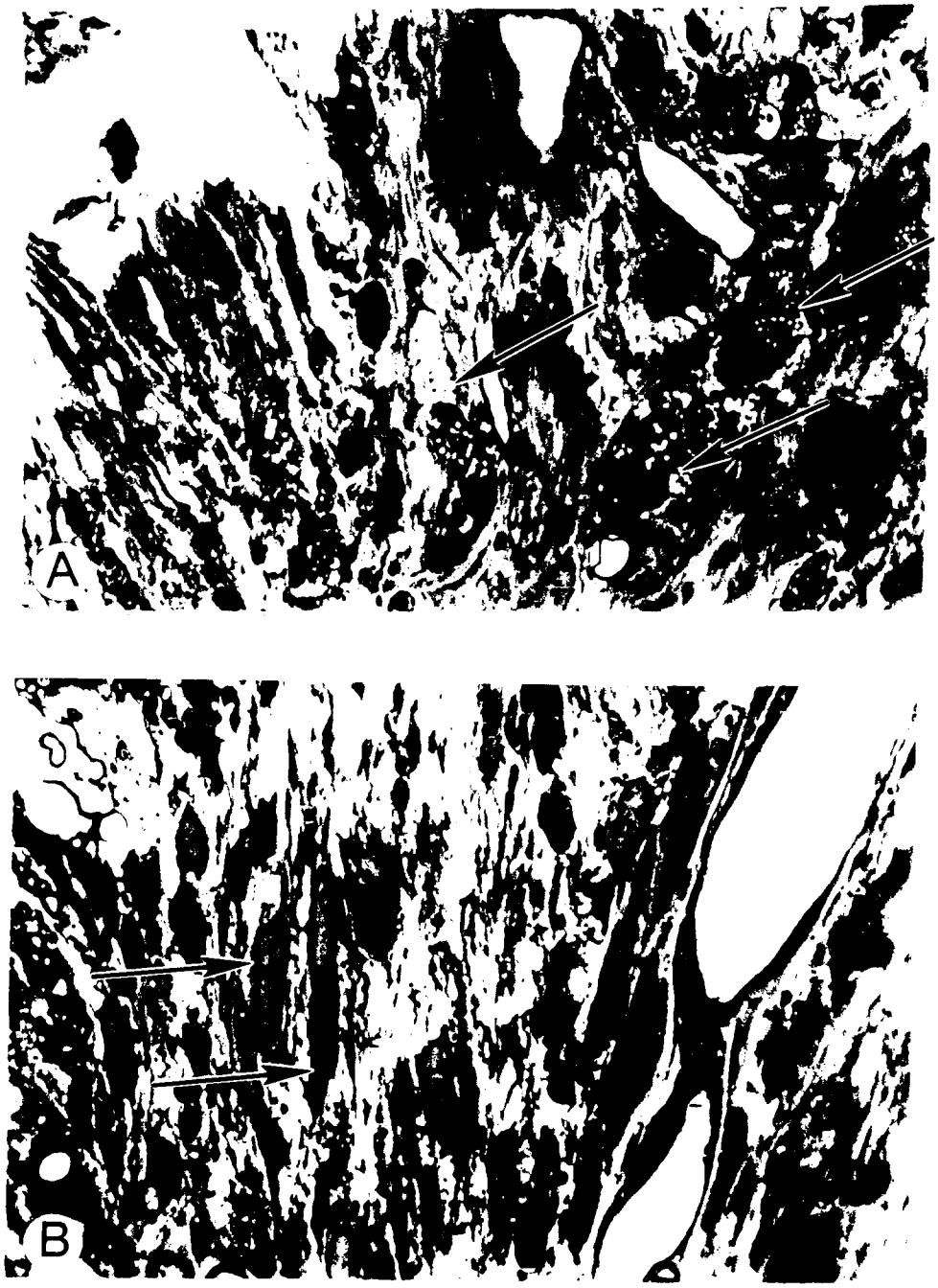

Fig. 9. SP-58, electrode 1. A. Macrophages (arrows) with vacuolar inclusions at the tip of the electrode. B. Scar lateral to the tip, containing elongated fibroblasts or glial cells (arrows) and increased extracellular space.

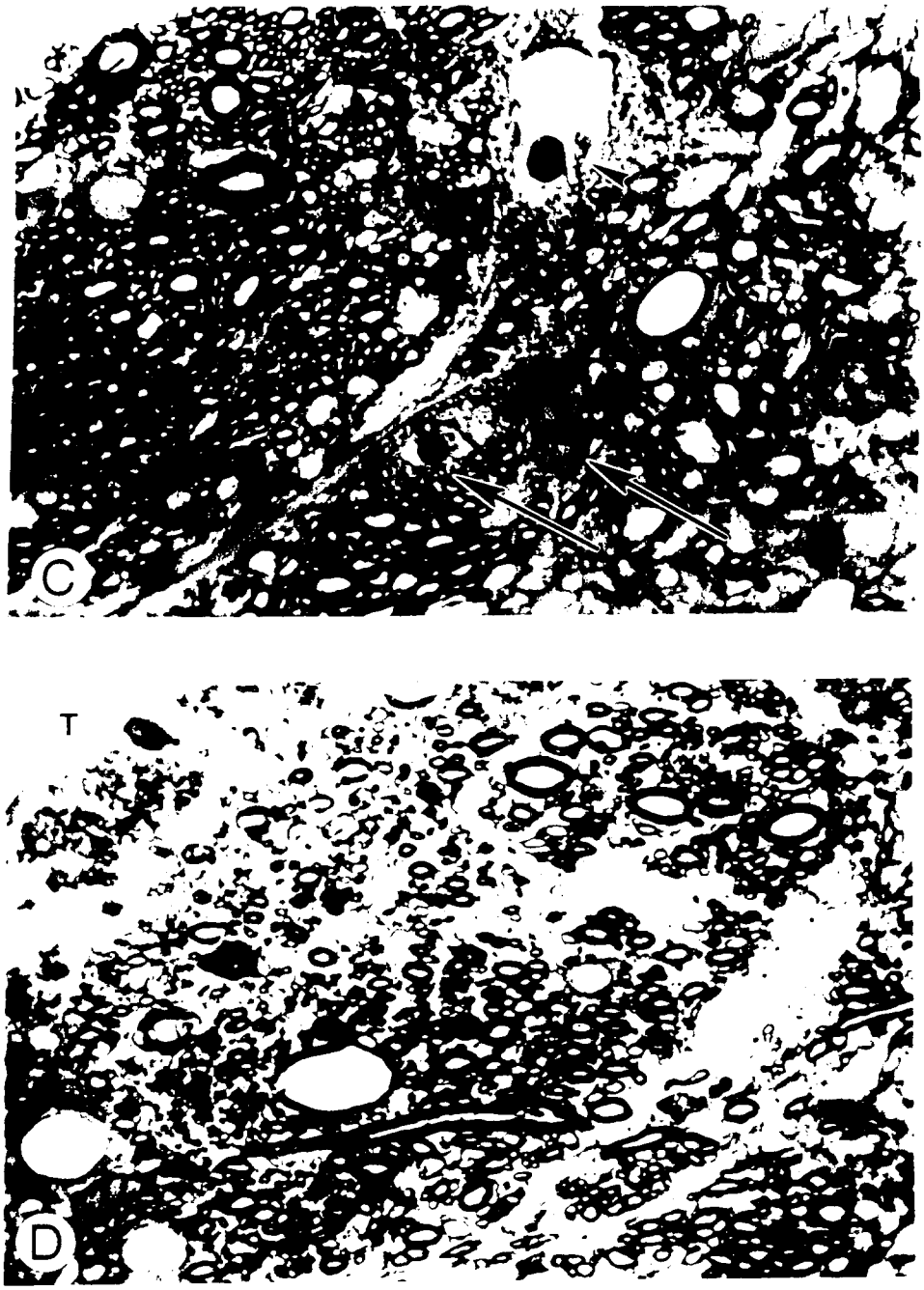

Fig. 9. C. Cell bodies (arrows) of the PPN, one of which is swollen (arrowhead). D. Portion of the lateral funiculus within the PPN. Note that the myelinated axons are of small caliber adjacent to the track (T). X 850.

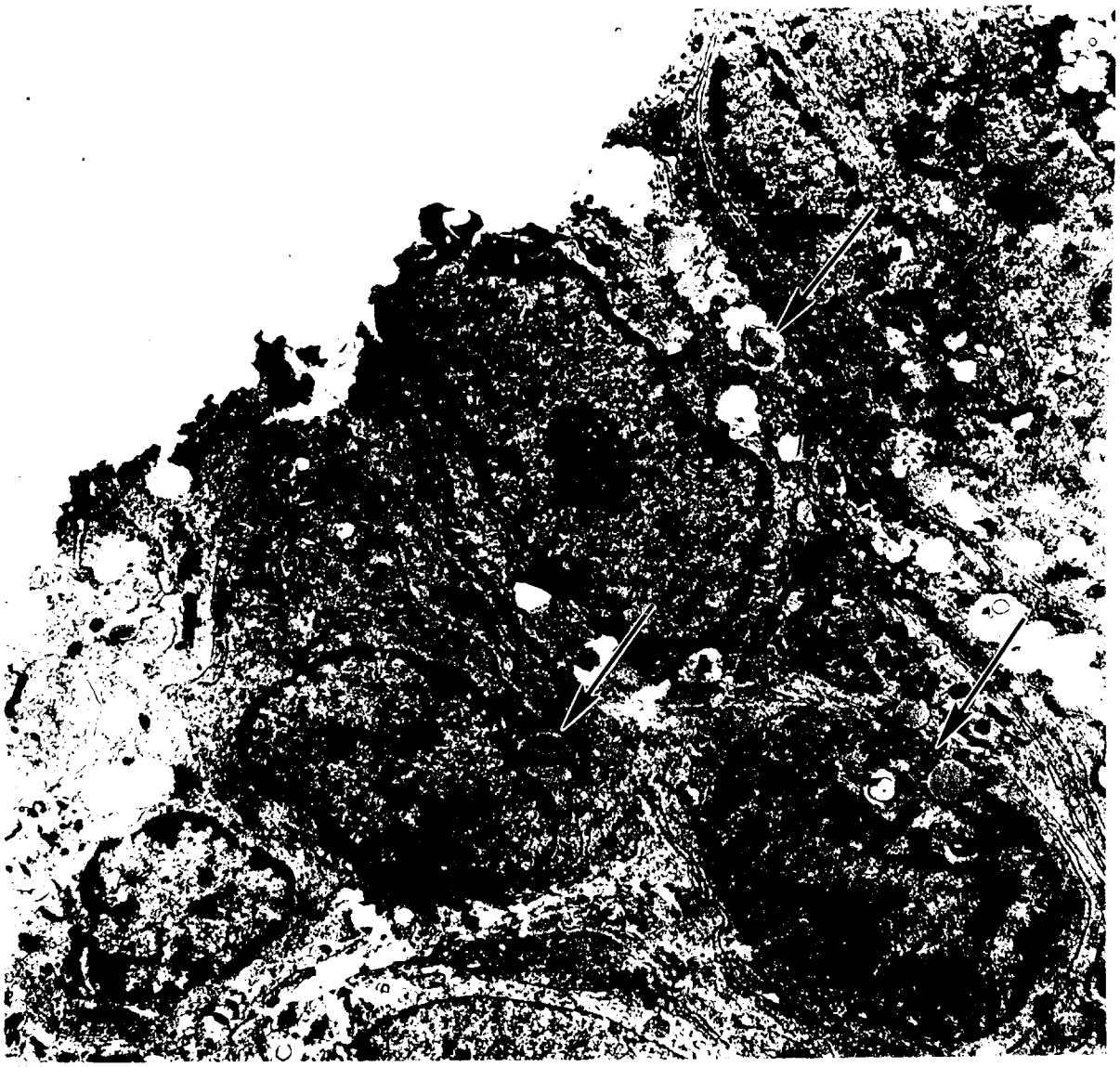

Fig. 10. Electron micrograph of cells at the tip of SP-58, electrode 1. These monocytic cells have numerous inclusions (arrows). X 6800.

Fig. 11. Electron micrograph of a blood vessel near the tip of electrode 1. The surrounding cells are actively phagocytic monocytes (arrows) and are presumed to be blood-borne. X 6,800.

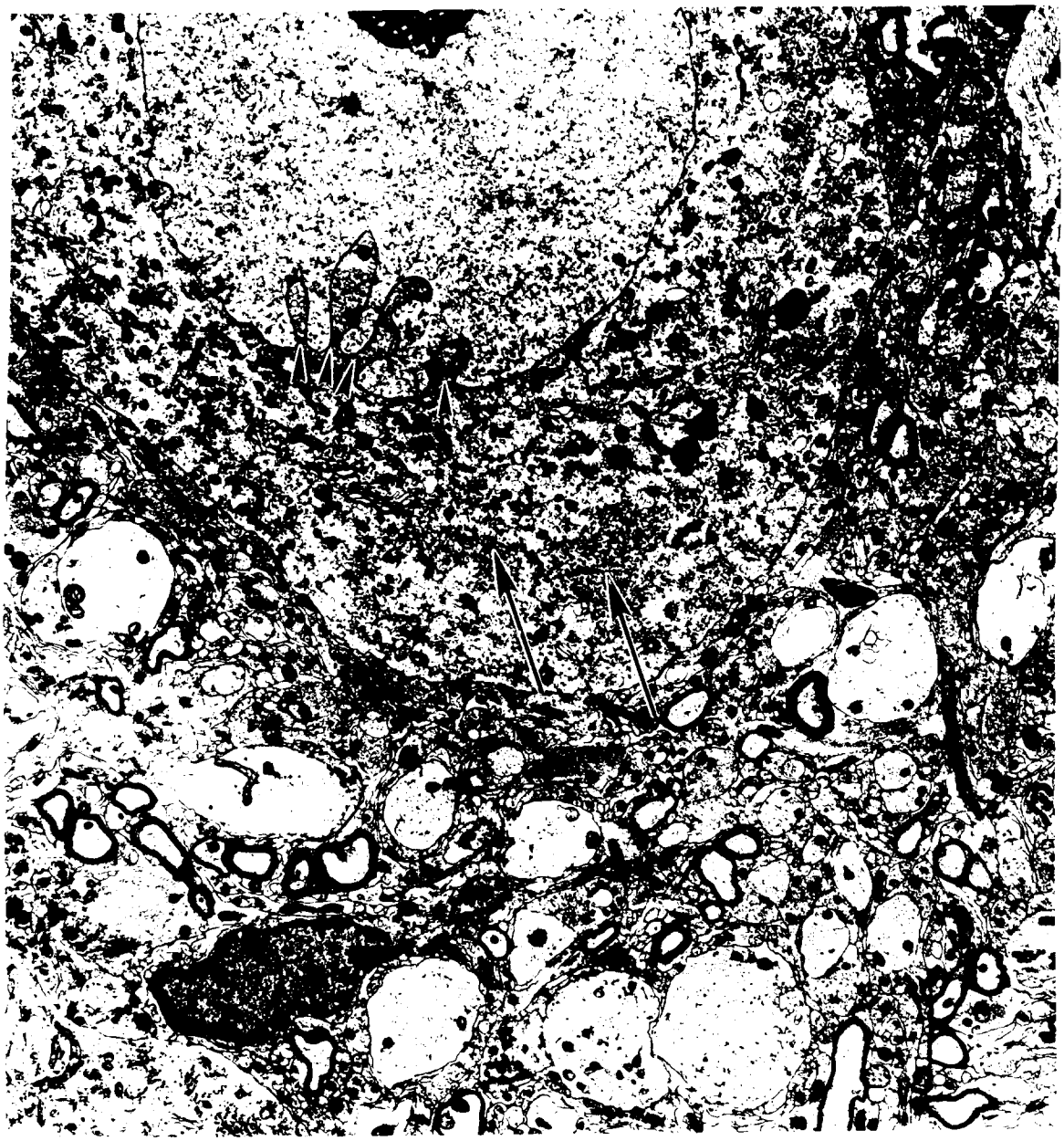

Fig. 12. Electron micrograph of a PPN cell near unpulsed electrode 1. Signs of chromatolysis include peripheral RER (arrows), indented nucleus (arrowheads) and filamentous cytoplasm. Dark lipofuscin granules are numerous. X 11,400.

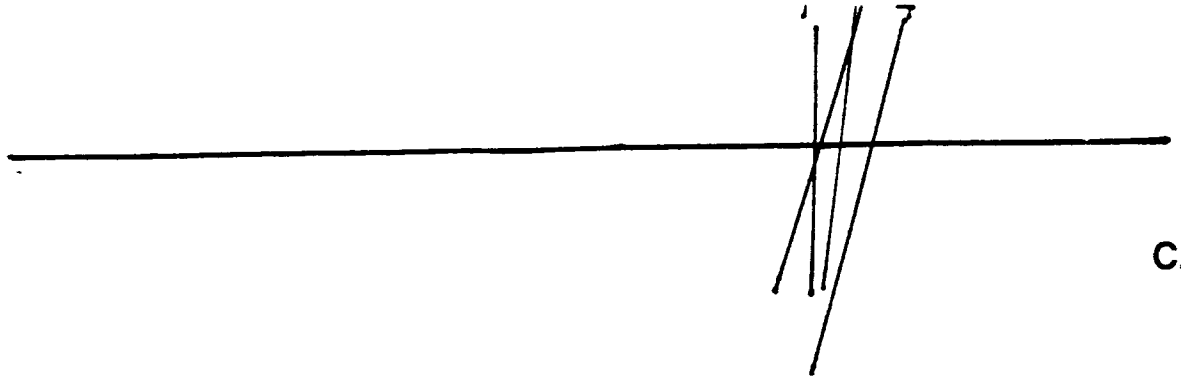

Longitudinal

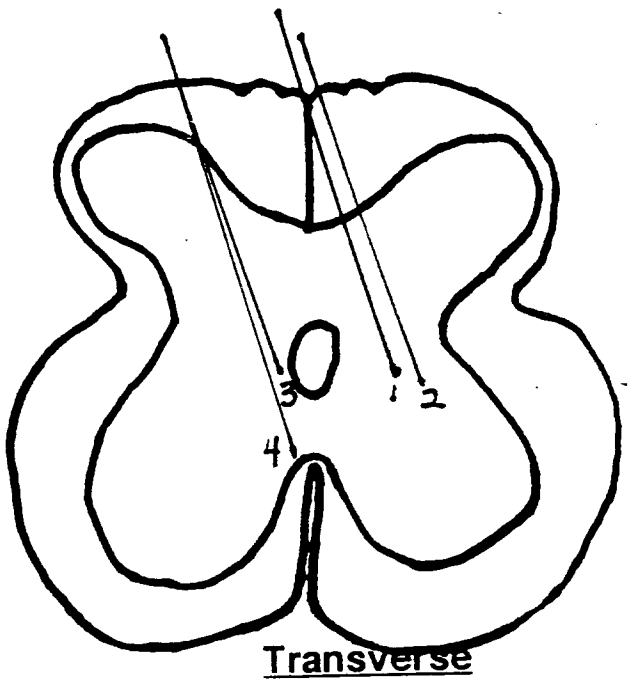

Transverse

B.

S2, SP61

A. Longitudinal reconstruction of location of electrode tracks in serial sections, showing rostral-caudal angles and tip depths. **B.** Transverse view of electrode tracks in serial sections, showing medial-lateral angles and tip positions in relation to PPN. Electrodes 1 and 3 were pulsed continuously.

Figure 13

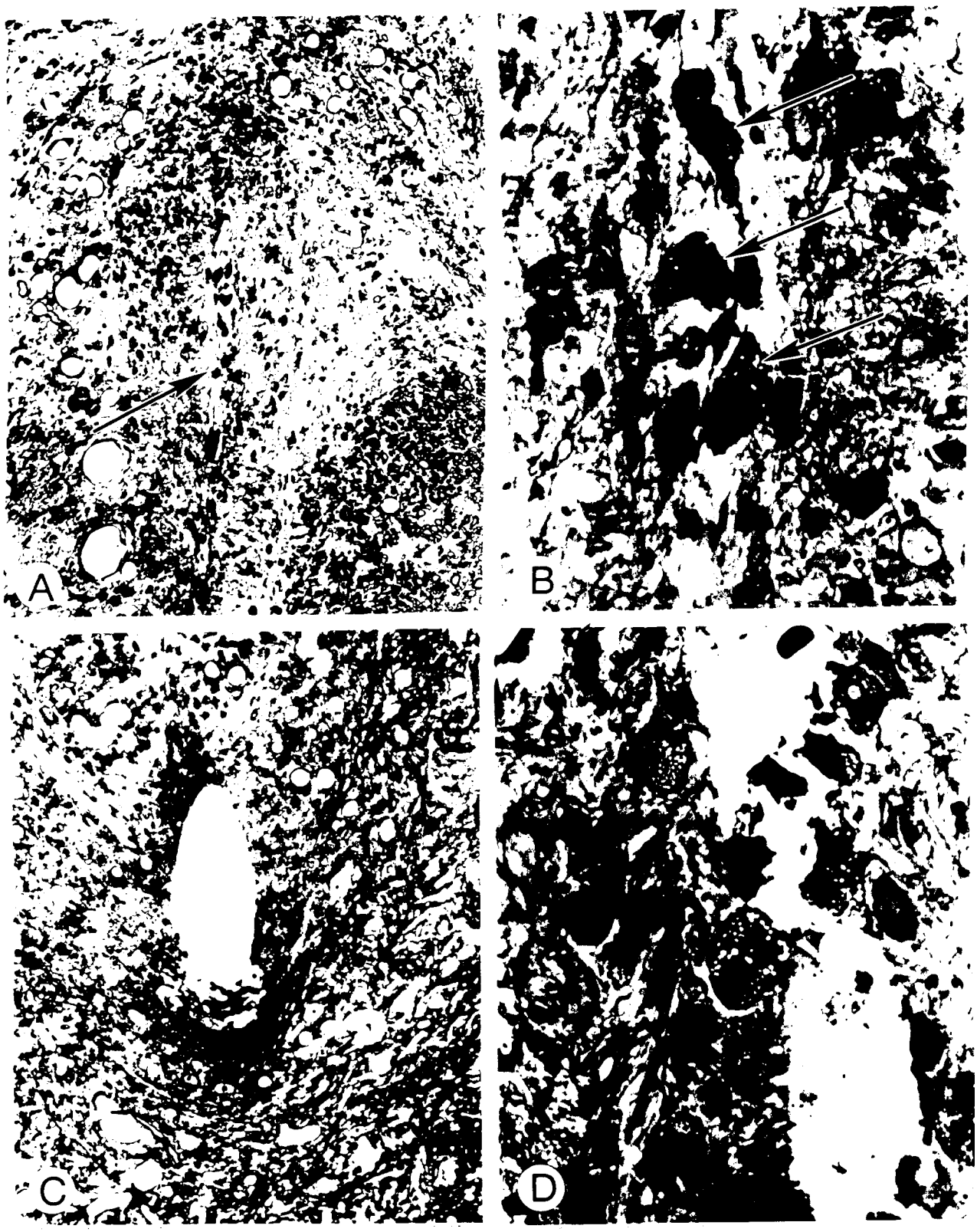

Fig. 14. SP-61. A and B. Tip of pulsed electrode 1 surrounded by many mononuclear cells. The track includes full-fledged macrophages (arrows). C and D. Tip of unpulsed electrode 2. Macrophages are adjacent to the track (arrows). A, X 85; B and D, X 850; C, X 340.

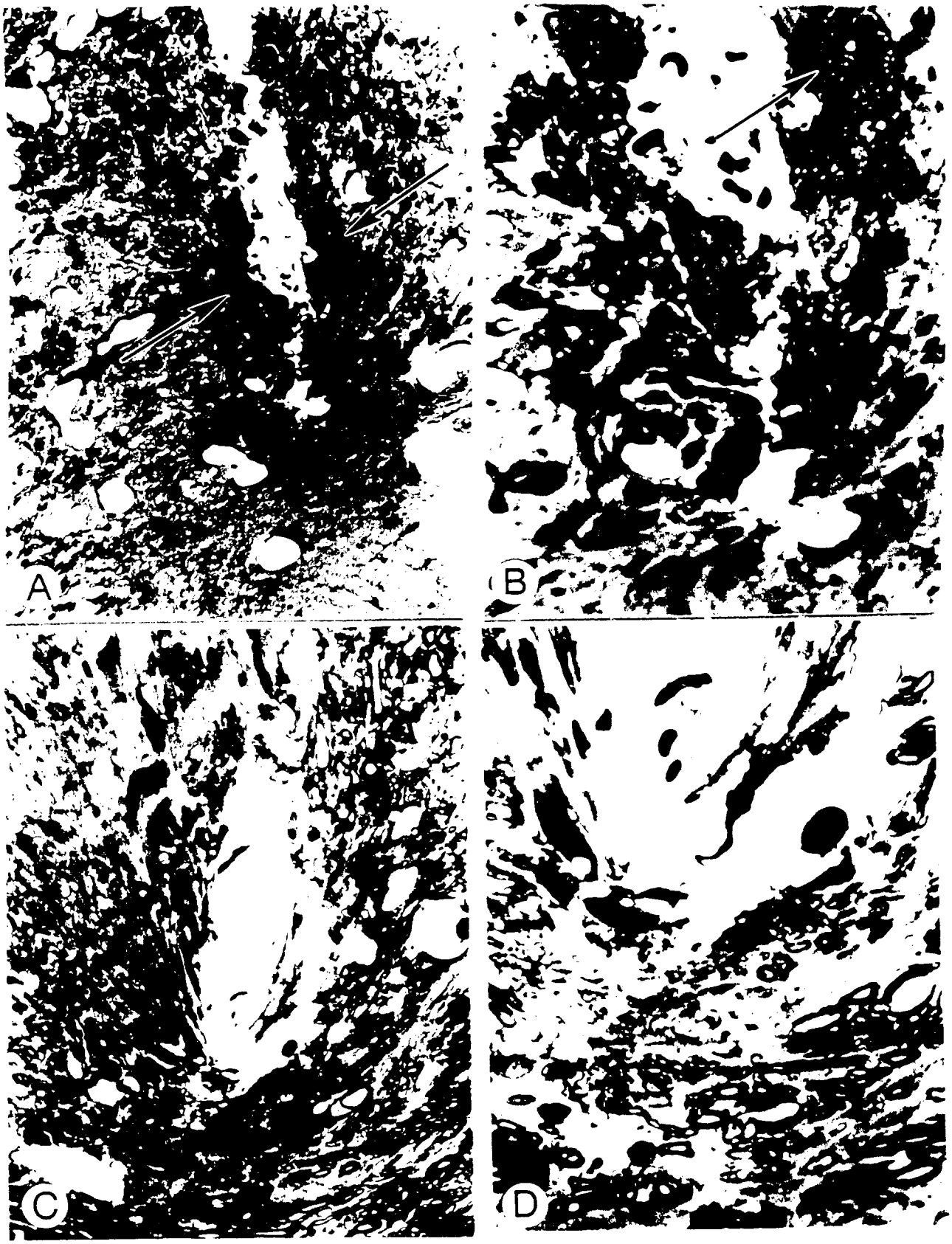

Fig. 15. SP-61. A and B. Tip of pulsed electrode 3 with numerous dark monocytes (arrows). At least one of these has inclusions (arrow in B). C and D. Tip of unpulsed electrode 4. This tissue has the appearance of gray matter in previously studied spinal cord with chronically implanted electrodes. A, X 340; B and D, X 850; C, X 170.

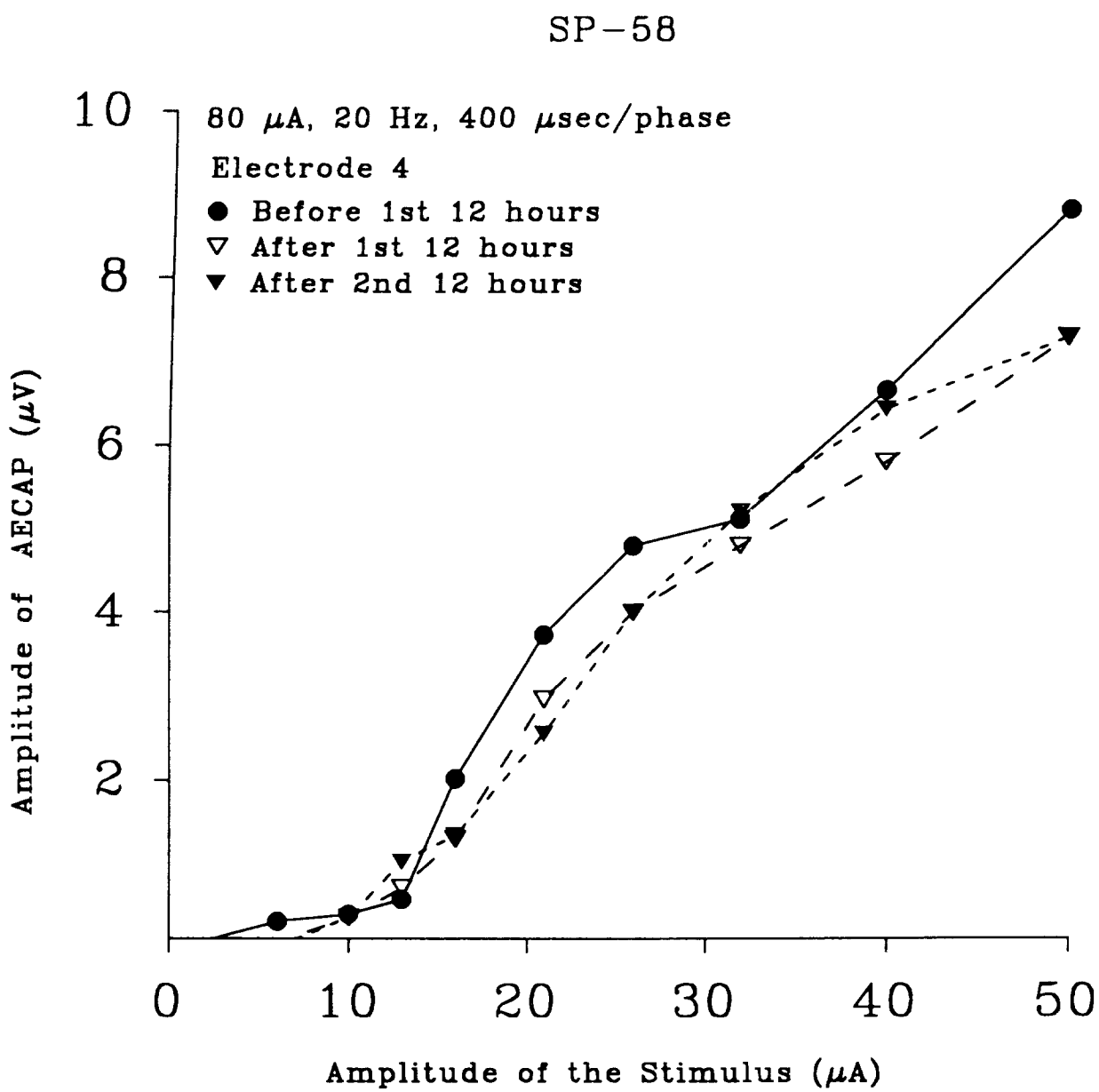

sp58a.spg

Fig. 16.

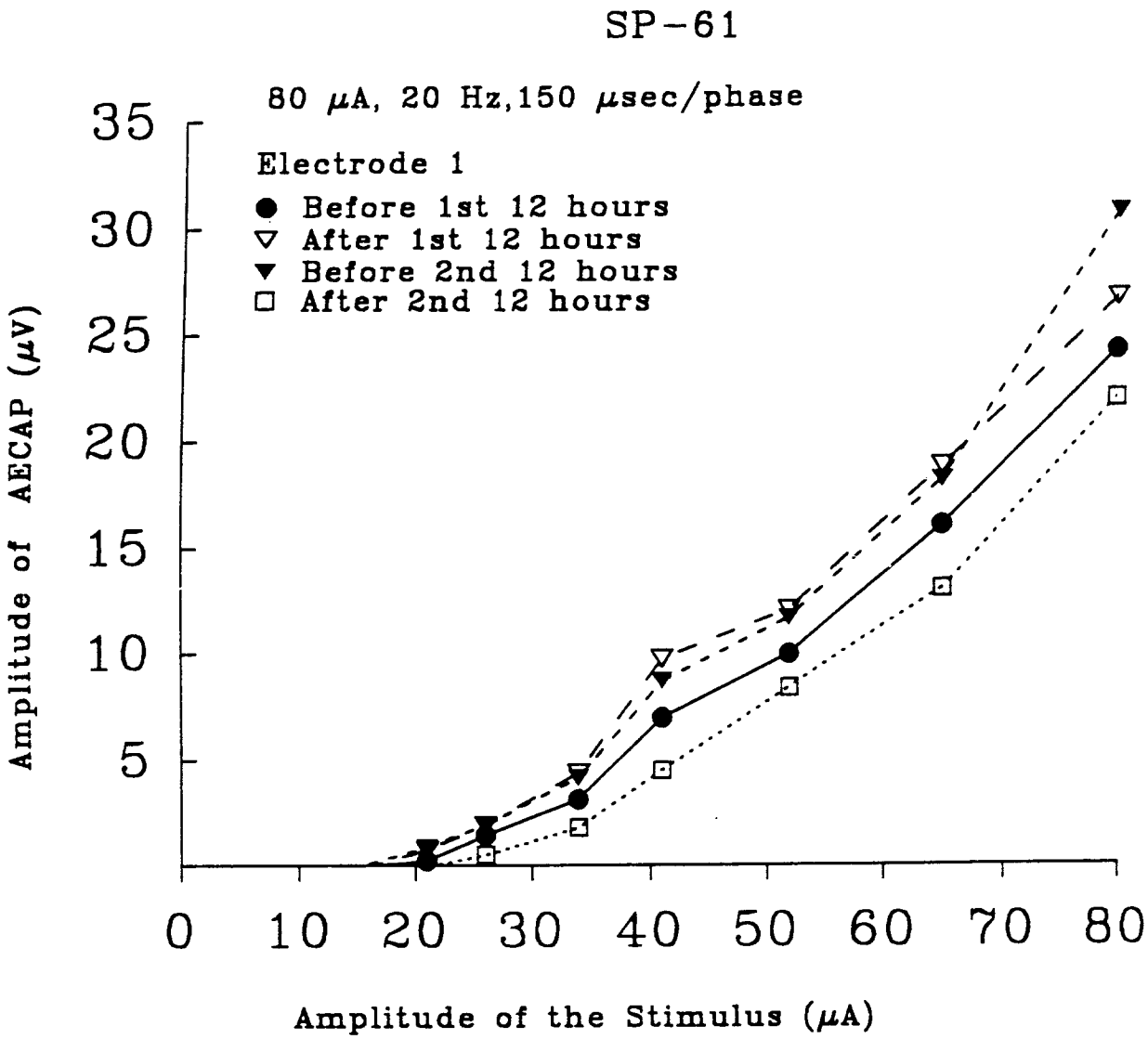

sp61b.spg

Fig. 17.

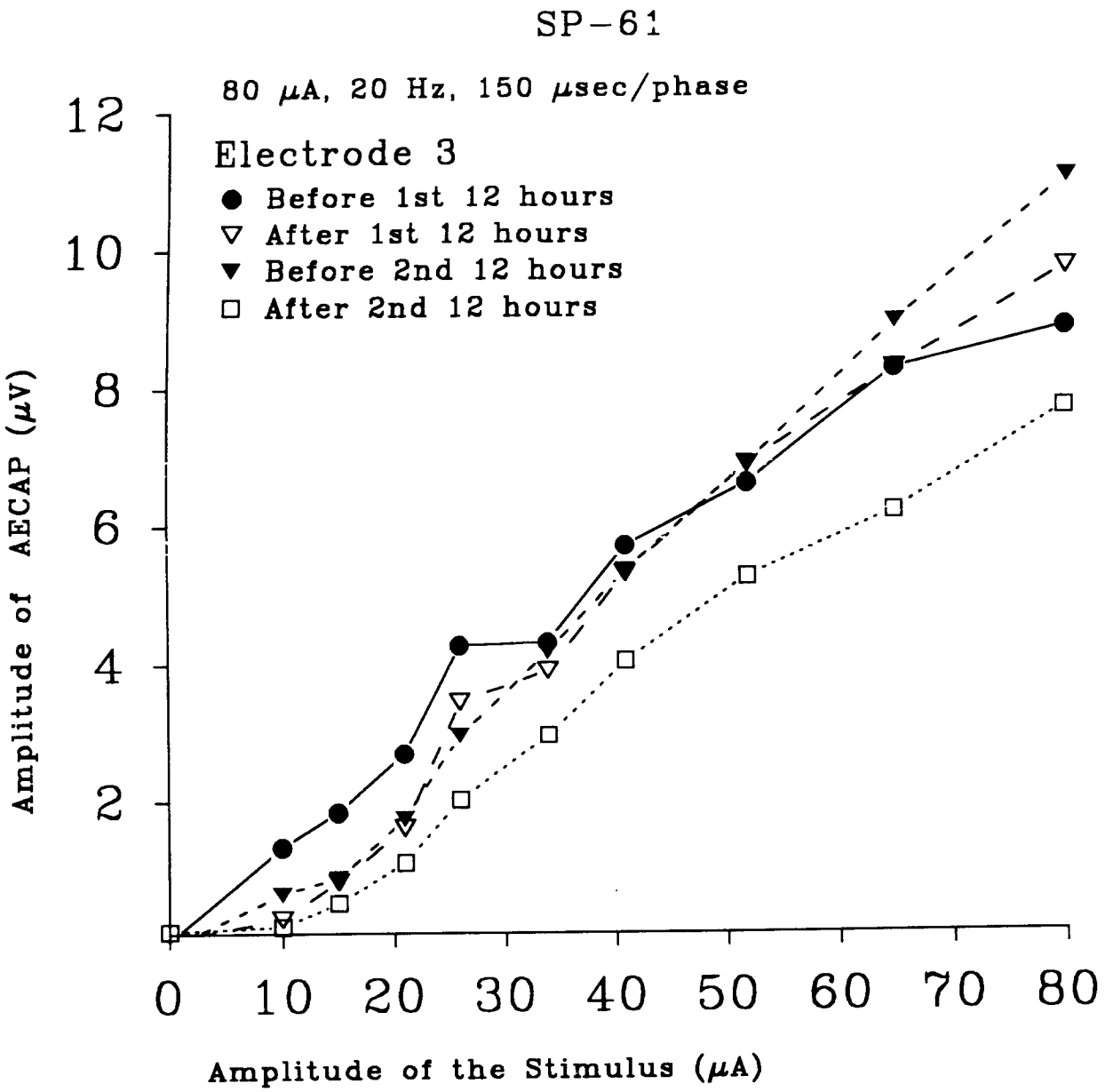

sp61c.spg

Fig. 18.

Fig. 19.

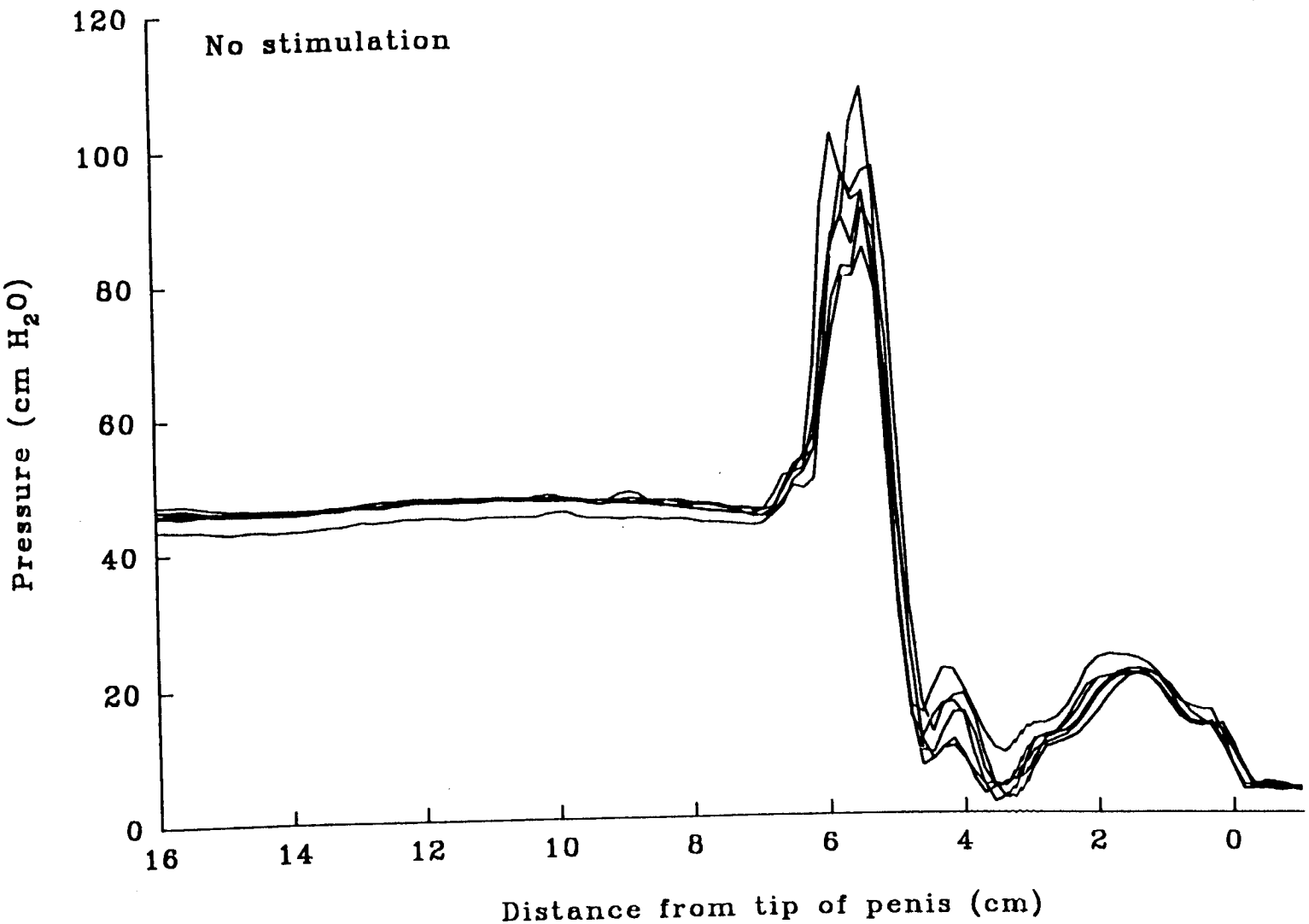

c:\plot41\spplots\sp64c.spg